

Local structure anomaly around Ge dopants in $\text{Mn}_3\text{Cu}_{0.7}\text{Ge}_{0.3}\text{N}$ with negative thermal expansion

J. Matsuno¹, K. Takenaka, H. Takagi¹, D. Matsumura, Y. Nishihata, and J. Mizuki

Citation: *Appl. Phys. Lett.* **94**, 181904 (2009); doi: 10.1063/1.3129169

View online: <http://dx.doi.org/10.1063/1.3129169>

View Table of Contents: <http://aip.scitation.org/toc/apl/94/18>

Published by the American Institute of Physics

Local structure anomaly around Ge dopants in $\text{Mn}_3\text{Cu}_{0.7}\text{Ge}_{0.3}\text{N}$ with negative thermal expansion

J. Matsuno,^{1,a)} K. Takenaka,^{1,2} H. Takagi,^{1,b)} D. Matsumura,³ Y. Nishihata,³ and J. Mizuki³

¹RIKEN (The Institute of Physical and Chemical Research), Wako, Saitama 351-0198, Japan

²Department of Crystalline Materials Science, Nagoya University, Nagoya 464-8603, Japan

³Synchrotron Radiation Research Center, Japan Atomic Energy Agency, Sayo-gun, Hyogo 679-5148, Japan

(Received 20 December 2008; accepted 14 April 2009; published online 5 May 2009)

Local structure analysis of Cu and Ge atoms in the negative thermal expansion material $\text{Mn}_3\text{Cu}_{0.7}\text{Ge}_{0.3}\text{N}$ was conducted using x-ray absorption fine structure measurements. The temperature dependence of the interatomic distance was found to reflect the macroscopic negative thermal expansion both for Cu–Mn and Ge–Mn shells, although the magnitude of the relative change was much larger for Ge–Mn than Cu–Mn. An enhanced anomaly of the Debye–Waller factor was observed for the Ge–Mn shell in the temperature region of the negative expansion, indicating the presence of static local disorder around Ge impurities. These local structure anomalies strongly suggest that the local and inhomogeneous strain around Ge is essential in broadening the discontinuous volume contraction. © 2009 American Institute of Physics. [DOI: 10.1063/1.3129169]

Negative thermal expansion (NTE) has been a subject of extensive studies due to its potential for technical applications where precise control of the thermal expansion is indispensable.^{1–4} Recently, giant NTE over a wide temperature range at around room temperature has been demonstrated in antiperovskite manganese nitrides Mn_3AN ($A=\text{Cu}$, Zn , Ga) doped with Ge or Sn.^{5–8} The pristine compound Mn_3AN ($A=\text{Zn}$ and Ga) often shows a large, discontinuous volume contraction of $\sim 2\%$ associated with a first-order transition from a low-temperature antiferromagnetic (AF) state to a high-temperature paramagnetic state.^{9–11} Recent neutron diffraction study indicates that the pronounced magnetovolume effect (MVE) in the Mn_3AN system occurs only when the noncollinear triangular Γ^{5g} spin structure is realized in the low temperature AF state, while the cubic crystal structure is maintained. This is very likely due to the presence of geometrical frustration inherent to the antiperovskite structure.¹²

In order to achieve a continuous MVE, it was necessary to dope the system. Ge and Sn were found to be effective dopants in broadening the sharp volume change over a certain temperature range. In contrast, other dopants maintain the width of the transition as sharp as the pristine compounds. It has been suggested that strong, local disorder around the Ge might give rise to the broadening of the discontinuous volume contraction.⁷ The importance of the doping effect on the coupling between lattice and magnetism is widely recognized as exemplified by the high magnetostriction in Fe doped with Ga.¹³ Here we report on local structure analysis of $\text{Mn}_3\text{Cu}_{0.7}\text{Ge}_{0.3}\text{N}$ using x-ray absorption fine structure (XAFS) measurements. XAFS is a powerful tool for probing the link between both thermal expansion and local structure through two important properties: interatomic distance (R) and a Debye–Waller factor (C_2), which is an index of the local disorder. XAFS measurements have also

been conducted for ZrW_2O_8 in connection with the origin of its NTE.¹⁴ We focused on the local structure around A site occupied by Cu and partially by Ge, probable source of local disorder, and coordinated with 12 Mn atoms. Local structure analysis of Ag-doped antiperovskite $\text{Mn}_3\text{Cu}_{0.7}\text{Ag}_{0.3}\text{N}$ was also conducted as a control experiment. $\text{Mn}_3\text{Cu}_{0.7}\text{Ag}_{0.3}\text{N}$ shows a large MVE around the same temperature as that of $\text{Mn}_3\text{Cu}_{0.7}\text{Ge}_{0.3}\text{N}$. In marked contrast to $\text{Mn}_3\text{Cu}_{0.7}\text{Ge}_{0.3}\text{N}$, the discontinuous volume contraction is maintained and, therefore, $\text{Mn}_3\text{Cu}_{0.7}\text{Ag}_{0.3}\text{N}$ does not function as an NTE material.

All of the measurements were performed using sintered polycrystalline samples made by solid-state reaction.^{5–7,15,16} Powders of Mn_2N and pure elemental A (purity of 99.9% or higher) were used as the starting materials. Linear thermal expansion $\Delta L(T)/L$ was measured using a strain gage (KYOWA; type KFL).⁵ XAFS measurements were carried out in transmission mode at bending-magnet beamline BL14B1 at SPring-8 using silicon (111) double crystal monochromator. Cu K edge (8.98 keV), Ge K edge (11.10 keV), and Ag K edge (25.52 keV) data were collected as a function of temperature from 15 to 300 K. The sample was mixed with a binder of BN and pressed into pellets for XAFS measurements. A simulation of all possible single and multiple scattering contributions was made using the FEFF 7.02 code.¹⁷

Linear thermal expansion of solid solution $\text{Mn}_3\text{Cu}_{1-x}\text{Ge}_x\text{N}$ (Ref. 5) and $\text{Mn}_3\text{Cu}_{1-x}\text{Ag}_x\text{N}$ are displayed in Fig. 1. While Mn_3CuN ($x=0$) does not show MVE unlike other Mn_3AN , doping of Ge or Ag induces a distinct MVE as observed in Mn_3ZnN at around $x=0.1$.¹⁸ Further doping of both Ag and Ge increases the transition temperature. However, from Fig. 1, Ge doping gives rise to not only the increase of transition temperature but also the broadening of the transition, particularly above $x=0.3$. This forms a contrast to Ag doping, where no appreciable broadening is observed up to $x=0.5$. We have carried out the local structure analysis of Ge- and Ag-doped compounds with the same doping level of $x=0.3$. At $x=0.3$, magnetic transition temperature T_N ($T_N=210$ K for Ge and 170 K for Ag) and the magnitude of the overall expansion associated with the tran-

^{a)}Electronic mail: matsuno@riken.jp.

^{b)}Also at Department of Advanced Materials Science, University of Tokyo, Kashiwa, Chiba 277-8561, Japan.

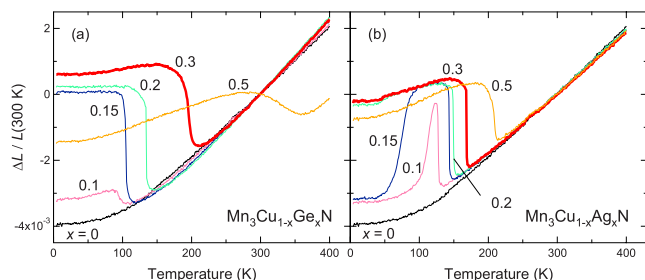


FIG. 1. (Color online) Linear thermal expansion of solid solution (a) $\text{Mn}_3\text{Cu}_{1-x}\text{Ge}_x\text{N}$ (Ref. 5) and (b) $\text{Mn}_3\text{Cu}_{1-x}\text{Ag}_x\text{N}$. Data was collected during cooling.

sition are comparable with each other. Nevertheless, the contrast in the broadening is already clear. This provides us with a good arena for clarifying the role of local structure and disorder in the mechanism of the broadening.

In order to demonstrate the quality of XAFS data, we show in Fig. 2(a) $k^2\chi(k)$ for Ge K edge in $\text{Mn}_3\text{Cu}_{0.7}\text{Ge}_{0.3}\text{N}$, where χ is an extended XAFS (EXAFS) function and k is a wave number of photoelectron. The Fourier transform (FT) of the EXAFS function is illustrated in Fig. 2(b). The Fourier transformation was made over the k range 3–13 \AA^{-1} at both the Cu K edge and the Ge K edge and 3–16 \AA^{-1} at the Ag K edge. In the 15 K data, one can recognize four peaks which correspond to different atomic shells around the central atom. By comparing with the simulated structure displayed in Fig. 2(c), each shell is assigned to Ge–Mn (1st), Ge–A (1st), Ge–Mn (2nd) and Ge–A (2nd) shells in ascending radius, respectively. Four peaks, which can be assigned in the same way as the Ge case, were also observed in the FT of the EXAFS function around Cu atoms in both $\text{Mn}_3\text{Cu}_{0.7}\text{Ge}_{0.3}\text{N}$ and $\text{Mn}_3\text{Cu}_{0.7}\text{Ag}_{0.3}\text{N}$ and Ag atoms in $\text{Mn}_3\text{Cu}_{0.7}\text{Ag}_{0.3}\text{N}$ (not shown). Such good agreement between the experiment and the simulation implies that the local structure around A site is close to what is expected from the average structure.

The local structure parameters, interatomic distances and Debye–Waller factors, were evaluated by nonlinear least squares fitting with anharmonic interatomic potentials for the first nearest neighbor of the A sites.¹⁹ The fitting procedure was as follows: the first-shell contributions were separated via Fourier filtering of the k^2 -weighted XAFS in the distance range 1.98–2.75 \AA for both the Ge K edge and the Cu K edge and 2.17–2.70 \AA for the Ag K edge. We have fitted

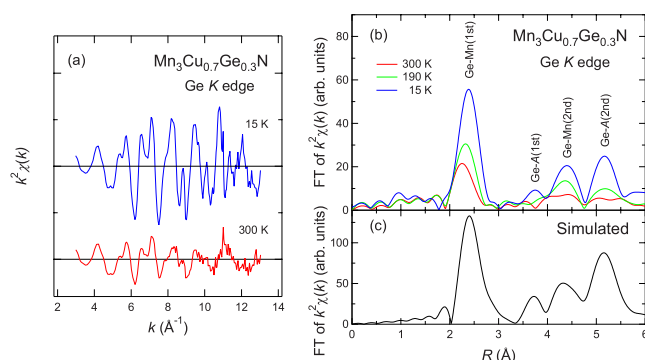


FIG. 2. (Color online) (a) k^2 -weighted EXAFS function $k^2\chi(k)$ for Ge K edge in $\text{Mn}_3\text{Cu}_{0.7}\text{Ge}_{0.3}\text{N}$. (b) FTs of $k^2\chi(k)$ for Ge K edge data at 15, 190, and 300 K, respectively. The phase shift of the photoelectron was not taken into account and hence neighbors appear closer to the x-ray absorbing atom than in the EXAFS function.

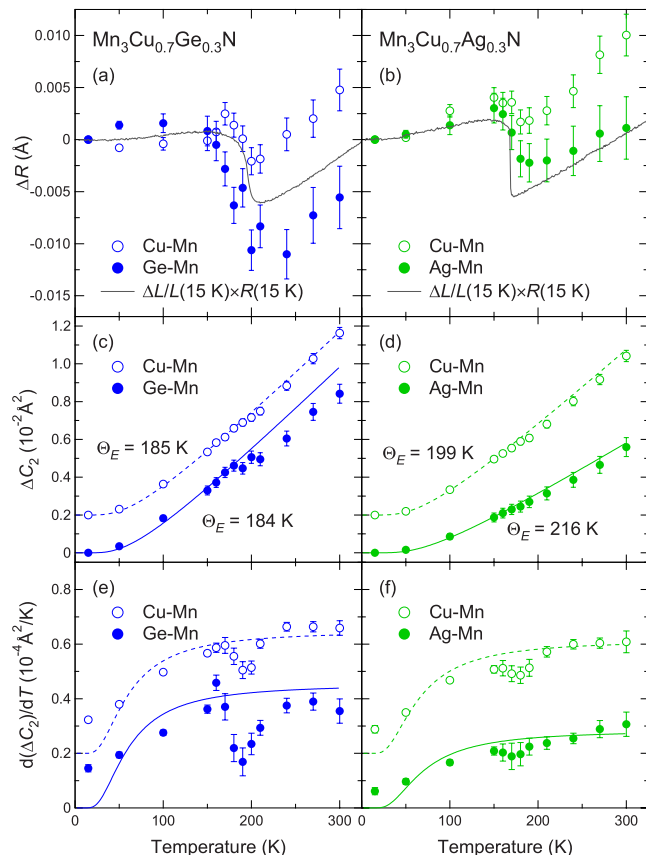


FIG. 3. (Color online) Temperature dependence of the relative interatomic distances (ΔR) for (a) $\text{Mn}_3\text{Cu}_{0.7}\text{Ge}_{0.3}\text{N}$ and (b) $\text{Mn}_3\text{Cu}_{0.7}\text{Ag}_{0.3}\text{N}$. For comparison, the linear thermal expansion $\Delta L/L$ multiplied by the interatomic distance A –Mn is also plotted. Temperature dependence of the relative Debye–Waller factors (ΔC_2) for (c) $\text{Mn}_3\text{Cu}_{0.7}\text{Ge}_{0.3}\text{N}$ and (d) $\text{Mn}_3\text{Cu}_{0.7}\text{Ag}_{0.3}\text{N}$. Temperature derivative of the Debye–Waller factors for (e) $\text{Mn}_3\text{Cu}_{0.7}\text{Ge}_{0.3}\text{N}$ and (f) $\text{Mn}_3\text{Cu}_{0.7}\text{Ag}_{0.3}\text{N}$. The data were smoothed in order to eliminate noises stemming from differential. Dotted and straight lines indicate the fitting with the Einstein model using the data below 150 K [(c) and (d)] and its derivative [(e) and (f)] for the Cu–Mn and Ge(Ag)–Mn shells, respectively (see text in detail). The data for the Cu–Mn shells are offset vertically for clarity.

backtransformed k -space data to 15 K data in order to determine the relative values of the interatomic distances and the Debye–Waller factors from the standard temperature of 15 K.

The results illustrate the anomalous local lattice distortion around the Ge dopant. Figure 3(a) demonstrates the temperature dependence of interatomic distances for the Cu–Mn and Ge–Mn shells in $\text{Mn}_3\text{Cu}_{0.7}\text{Ge}_{0.3}\text{N}$. It is clear that the interatomic distances for both the Cu–Mn and the Ge–Mn shell mirror the bulk volume contraction (NTE), showing a clear contraction in the temperature region where NTE is observed. A similar but much less pronounced contrast between Cu and Ag is seen for $\text{Mn}_3\text{Cu}_{0.7}\text{Ag}_{0.3}\text{N}$ [Fig. 3(b)]. The large structural changes around the dopants in both systems might reflect the fact that the MVE is triggered by the dopants in Mn_3CuN system. Taking into account of the similar magnitude of the overall negative expansion in both compounds, the contrast between Ge and Ag suggests that the Ge dopants induce more intense local strain in their surroundings than the Ag dopants. It is worth noting that this local structure is not related to the average structure. The cubic lattice constants at room temperature are 3.900, 3.942, and 3.908 \AA , for $\text{Mn}_3\text{Cu}_{0.7}\text{Ge}_{0.3}\text{N}$, $\text{Mn}_3\text{Cu}_{0.7}\text{Ag}_{0.3}\text{N}$, and

Mn₃CuN, respectively, manifesting that the change in the lattice constants upon doping is larger in Ag than in Ge. This local strain, unique to the Ge dopant, might be one of the key factors of the broadening of the sharp volume contraction.

In Figs. 3(c) and 3(d), the Debye–Waller factors for Mn₃Cu_{0.7}Ge_{0.3}N and Mn₃Cu_{0.7}Ag_{0.3}N are shown, respectively. In general, the Debye–Waller factor consists of two contributions: (i) dynamic (or thermal) vibration and (ii) static local disorder. The overall increase of the Debye–Waller factor with temperature, observed for both Cu–Mn and Ge–Mn in Mn₃Cu_{0.7}Ge_{0.3}N and for Cu–Mn and Ag–Mn in Mn₃Cu_{0.7}Ag_{0.3}N, can be attributed to the increase of the thermal vibrations. Focusing on the details, however, we observe an anomaly in the temperature dependence of the Debye–Waller factor around the temperature region of the NTE. In order to extract the anomaly from the overall increase, we have fitted the data below 150 K with the Einstein model, assuming that the temperature (T) dependence of the Debye–Waller factor (C_2) for first shells can be denoted as $C_2 = (\hbar^2/2\mu k_B \Theta_E) \coth(\Theta_E/2T)$, where μ is the reduced mass, k_B Boltzmann constant, \hbar Planck constant, and Θ_E the Einstein temperature. The reduced masses are calculated using atomic masses of Mn, Cu, Ge, and Ag. The only fitting parameter is Θ_E as displayed in Figs. 3(c) and 3(d). The Einstein temperature is quite similar among the four data, implying that the rigidity of bond is not very different. On the other hand, the deviation from the fitted line is pronounced above 150 K especially in the Ge–Mn shell for Mn₃Cu_{0.7}Ge_{0.3}N, indicating that the anomaly of the Debye–Waller factor is most striking around Ge dopants.

In order to see this anomaly more clearly, we show in Figs. 3(e) and 3(f) the temperature derivative of the Debye–Waller factors. For both systems, we clearly see a dip structure around the temperature range of NTE. The dip is more pronounced for Mn₃Cu_{0.7}Ge_{0.3}N (broad MVE) than for Mn₃Cu_{0.7}Ag_{0.3}N (sharp MVE). It is notable that the largest drop is observed for the Ge–Mn shell indicating again the unique local structure around Ge dopants. The dip in the derivative implies an increase of the effective Debye–Waller factor upon cooling in the NTE region. Assuming that the contribution is only from dynamic vibration, this would correspond to the softening of the phonon. Since the Cu, Ag, and Ge dopants occupy the same site, it is not natural to have softening only around the Ge dopants. We therefore believe that the anomaly of the Debye–Waller factor in the NTE region, particularly pronounced for the Ge–Mn shell, represents the static disorder; the broadened MVE is accompanied with a pronounced local disorder around the Ge dopants. Although we cannot reconstruct a full local structure from the XAFS data, this local disorder might be related to the rotation of NMn₆ octahedra which was very recently observed in Mn₃Cu_{1-x}Ge_xN by neutron pair distribution function analysis.²⁰

The uniqueness of Ge as a dopant is represented by its intense local strain and static local disorder, the roles of which have been unrecognized in the physics of NTE materials based on itinerant-electron magnetism. At present it is an open question how the local character of the Ge dopant microscopically relax the MVE. We speculate that the combination of the intense strain and disorder around the Ge

dopant may impose local inhomogeneity on surroundings. Since the MVE is highly sensitive to the strain, the strong inhomogeneity caused by the disorder-induced strain tends to suppress the phase transition of the whole system. If the effect of inhomogeneity is enhanced by a cooperative effect between the dopants at certain doping levels, it may lead to the macroscopic relaxation of the MVE; the system might be viewed as a magnetovolume relaxor in analogy with ferroelectric relaxor.

In summary, we have analyzed the local structure of Mn₃Cu_{0.7}Ge_{0.3}N with negative thermal expansion by XAFS. In comparison with the Ag dopant in Mn₃Cu_{0.7}Ag_{0.3}N that displays no broadening of the discontinuous volume contraction, the Ge dopant was found to cause the intense local strain and the local disorder around it. Our findings shed light on the fact that the local strain and disorder carry the advantage of the Ge dopant and likely broaden the sharp magnetovolume effect. We believe that this is the key ingredient for the negative thermal expansion in the Mn₃AN system.

The authors thank A. Fujita, Y. Nakamura, R. S. Perry, S. Iikubo, K. Kodama, and S. Shamoto for valuable discussions. This work was partly supported by Industrial Technology Research Grant Program from NEDO, Japan. This work was performed under the Common-Use Facility Program of JAEA.

¹A. W. Sleight, *Inorg. Chem.* **37**, 2854 (1998).

²J. S. O. Evans, *J. Chem. Soc. Dalton Trans.* **1999**, 3317.

³G. D. Barrera, J. A. O. Bruno, T. H. K. Barron, and N. L. Allan, *J. Phys.: Condens. Matter* **17**, R217 (2005).

⁴A. E. Phillips, A. L. Goodwin, G. J. Halder, P. D. Southon, and C. J. Kepert, *Angew. Chem., Int. Ed.* **47**, 1396 (2008).

⁵K. Takenaka and H. Takagi, *Appl. Phys. Lett.* **87**, 261902 (2005).

⁶K. Takenaka and H. Takagi, *Mater. Trans.* **47**, 471 (2006).

⁷K. Takenaka, K. Asano, M. Misawa, and H. Takagi, *Appl. Phys. Lett.* **92**, 011927 (2008).

⁸R. Huang, L. Li, F. Cai, X. Xu, and L. Qian, *Appl. Phys. Lett.* **93**, 081902 (2008).

⁹For a review, see D. Fruchart and E. F. Bertaut, *J. Phys. Soc. Jpn.* **44**, 781 (1978).

¹⁰R. Fruchart, R. Madar, M. Barberon, E. Fruchart, and M. G. Lorthioir, *J. Phys. Colloq.* **32**, C1-982 (1971).

¹¹Ph. l'Heritier, D. Boursier, R. Fruchart, and D. Fruchart, *Mater. Res. Bull.* **14**, 1203 (1979).

¹²S. Iikubo, K. Kodama, K. Takenaka, H. Takagi, and S. Shamoto, *Phys. Rev. B* **77**, 020409R (2008).

¹³A. E. Clark, J. B. Restorff, M. Wun-Fogle, T. A. Lograsso, and D. L. Schlagel, *IEEE Trans. Magn.* **36**, 3238 (2000).

¹⁴D. Cao, F. Bridges, G. R. Kowach, and A. P. Ramirez, *Phys. Rev. Lett.* **89**, 215902 (2002).

¹⁵W. S. Kim, E. O. Chi, J. C. Kim, N. H. Hur, K. W. Lee, and Y. N. Choi, *Phys. Rev. B* **68**, 172402 (2003).

¹⁶T. Kaneko, T. Kanomata, and K. Shirakawa, *J. Phys. Soc. Jpn.* **56**, 4047 (1987).

¹⁷S. I. Zabinsky, J. J. Rehr, A. Ankudinov, R. C. Albers, and M. J. Eller, *Phys. Rev. B* **52**, 2995 (1995).

¹⁸The Ag-doped samples with $x=0.1$ and 0.15 show the lower-temperature phase transition in addition to the MVE. This extra transition is known to be a magnetic transition of which the origin is beyond the subject of the present paper.

¹⁹T. Yokoyama, H. Hamamatsu and T. Ohta, EXAFSH 2.4, The University of Tokyo, 1998.

²⁰S. Iikubo, K. Kodama, K. Takenaka, H. Takagi, M. Takigawa, and S. Shamoto, *Phys. Rev. Lett.* **101**, 205901 (2008).